The effect of electric fields on Ag(001) $c(2 \times 2)$-Xe

1998 J. Phys.: Condens. Matter 10 7777

(http://iopscience.iop.org/0953-8984/10/35/011)

J. Phys.: Condens. Matter **10** (1998) 7777–7792. Printed in the UK PII: S0953-8984(98)93709-2

The effect of electric fields on Ag(001) c(2 × 2)–Xe

S Clarke†, M Nekovee‡, P K de Boer§ and J E Inglesfield†

† Department of Physics and Astronomy, University of Wales Cardiff, PO Box 913, Cardiff CF2 3YB, UK

‡ Department of Physics, The Blackett Laboratory, Imperial College, London SW7 2BZ, UK

§ Department of Physics, University of Nijmegen, Toernooiveld, NL-6525 ED Nijmegen, The Netherlands

Received 24 April 1998, in final form 8 July 1998

Abstract. The electronic structure of Ag(001) with an adsorbed overlayer of Xe is calculated in external electric fields of varying strength. The screening mostly takes place on the top of the surface Ag atoms, with polarization of the Xe atom. The variation in the centroid of the screening charge (the image plane) with field strength is studied, and it is found that the adsorption of Xe reduces the non-linear response compared with that of the clean Ag surface. The distribution of screening charge between the various atoms is found using a generalized effective charge, and it is found that the screening charge on Ag atoms directly underneath Xe is enhanced. The generalized effective charge gives the derivative of the force at the surface with respect to the electric field, and the phenomena of field-induced chemisorption and field desorption are discussed in these terms.

1. Introduction

In recent times there has been much interest in the effect of electric fields upon metal surfaces especially when these surfaces have adsorbates upon them. The initial motivation for this interest was to provide a greater understanding of field evaporation and desorption and to look at field-induced adsorption (enhanced binding of adsorbates in the presence of electric fields) [1, 2]. Much of the research in this area has also resulted from the need to better understand the processes occurring in electrolytic cells where the large fields at the electrodes affect the surface electronic structure. Recently, however, interest has been generated in this subject by another application, the manipulation of single adsorbate atoms using an STM tip [3]; clearly this has applications to the growing area of nanotechnology, opening up the possibility of building wires and other components atom by atom. A related discovery which is also fuelling the interest in these systems is the 'atomic switch' [4] in which an adsorbate atom can be made to jump between the substrate and STM tip and then back again by application of suitable fields.

Initial work on inert-gas adsorbates on metals was largely carried out by the field emission community with the majority of calculations using simple models to look at field emission for example [5–7]. More recently, first-principles calculations for adsorbates on jellium surfaces have been carried out using the method of Lang [40]. These calculations have led to an understanding of the effect of adsorbates and electric fields on the electronic structure of metal surfaces as well as a better understanding of the energetics involved in the processes that occur at these interfaces. The jellium calculations cannot however reproduce effects arising from the atomistic nature of the charge density at the metal surface,

0953-8984/98/357777+16$19.50

such as field enhancement around the atoms. To stand any chance of getting a complete understanding of the processes involved we need self-consistent full-potential calculations. In this work we present the results of self-consistent calculations incorporating the full crystal potential for Ag(001)c(2×2)–Xe in the presence of an external electric field using the embedding method [8] to take care of the semi-infinite substrate. This is a particularly interesting system, because it has been suggested that Xe, unlike the lighter rare-gas atoms, shows some chemisorption. Moreover Xe is widely studied in connection with the atomic switch.

The embedding method [8] which we use is described in section 2. It handles situations where a localized perturbation in an extended system reduces the symmetry of the system. An example of this is in calculations like those presented here where the surface reduces the symmetry of the perfect infinite crystal. It is clearly desirable to just solve the Schrödinger equation in the region of interest which is usually in the vicinity of the perturbation—the top few atomic layers. Evidently there is coupling between this region and the rest of the extended system so we have to find a way of taking this coupling into account. Using the embedding method, we can proceed by solving the Schrödinger equation explicitly only in the surface region. The coupling of the wavefunctions in this region to those in the bulk is incorporated by means of an energy-dependent non-local embedding potential (defined on the boundary between the surface region and the bulk) derived from the bulk Green function. What this means is that with the embedding potential included in the surface region Hamiltonian, we can solve the Schrödinger equation just in this region, whilst implicitly including the influence of the rest of the crystal and hence performing a calculation for the true semi-infinite system.

In section 3 we present our results for the field-free electronic structure of the Xe–Ag system, discussing the density of states, workfunction and self-consistent charge density. Then in section 4 we show the effect of an applied external field on this electronic structure, obtaining values for the position of the static image plane and making a comparison with classical electrostatics. We shall also consider the field dependence of the static image plane which is relevant to second-harmonic generation and its change with Xe adsorption. The

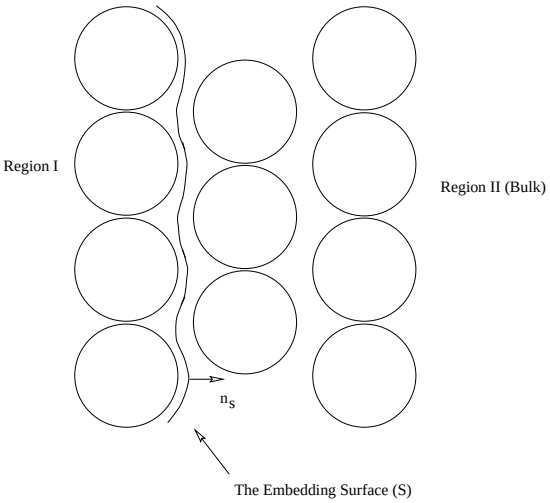

Figure 1. The embedding geometry in a surface embedded Green function calculation, region I being the surface layers and region II being the bulk crystal.

concept of effective charge is being increasingly used as it provides a unique definition of the charge on an atom and gives the force on the atom in an external electric field [9]. In section 5 we introduce a generalization of this concept to arbitrary fields and use it to study the effect of the applied electric field on the bonding between the Xe adsorbates and the Ag substrate. The information gained is then used to consider the mechanisms responsible for the effects apparent in the Eigler atomic switch.

2. Computational method

We partition the semi-infinite system into two parts, the surface (region I) and the substrate (region II), as shown in figure 1. In the embedding method, a variational principle is given for the energy in terms of a trial function ϕ defined only in region I; all of the contributions coming from matching this solution and the substrate wavefunctions are contained in the embedding potential G_0^{-1}. This variational principle (which is given in atomic units which are used throughout this paper with $\hbar = e = m = 1$) is given by

$$E = \left(\int_I \mathrm{d}^3\boldsymbol{r}\ \phi^* H \phi + \frac{1}{2}\int_S \mathrm{d}^2\boldsymbol{r}_s\ \phi^* \frac{\partial \phi}{\partial \boldsymbol{n}_s} + \int_S \mathrm{d}^2\boldsymbol{r}_S \int_S \mathrm{d}^2\boldsymbol{r}'_S\ \phi^*(\boldsymbol{r}_s)\left[G_0^{-1} - \epsilon \frac{\partial G_0^{-1}}{\partial E}\right]\phi(\boldsymbol{r}'_S)\right) \times \left(\int_I \mathrm{d}^3\boldsymbol{r}\ |\phi|^2 - \int_S \mathrm{d}^2\boldsymbol{r}_S \int_S \mathrm{d}^2\boldsymbol{r}'_S\ \phi^*(\boldsymbol{r}_S)\frac{\partial G_0^{-1}}{\partial E}\phi(\boldsymbol{r}'_s)\right)^{-1}. \tag{1}$$

G_0^{-1}, which depends only on the substrate Green function, is evaluated at some trial energy ϵ, and the energy derivative terms provide a first-order correction to give it at the right energy. The embedding potential is in fact a generalized logarithmic derivative which ensures that the solution in region I matches in amplitude and derivative onto the substrate wavefunctions.

To proceed with minimizing E let us now expand ϕ in a set of basis functions:

$$\phi(\boldsymbol{r}) = \sum_i a_i \chi_i(\boldsymbol{r}). \tag{2}$$

This leads to the following matrix equation for the coefficients a_j:

$$\sum_j \left[H_{ij} + (G_0^{-1})_{ij} + (E-\epsilon)\frac{\partial (G_0^{-1})_{ij}}{\partial E}\right] a_j = E \sum_j O_{ij} a_j \tag{3}$$

where

$$\begin{aligned} H_{ij} &= \int_I \mathrm{d}^3\boldsymbol{r}\ \chi_i^*(\boldsymbol{r}) H \chi_j(\boldsymbol{r}) + \frac{1}{2}\int_S \mathrm{d}^2\boldsymbol{r}_S\ \chi_i^* \frac{\partial \chi_j}{\partial \boldsymbol{n}_s} \\ (G_0^{-1})_{ij} &= \int_S \mathrm{d}^2\boldsymbol{r}_s \int_S \mathrm{d}^2\boldsymbol{r}'_s\ \chi_i^*(\boldsymbol{r}_s) G_0^{-1}(\boldsymbol{r}_s, \boldsymbol{r}'_s)\chi_j(\boldsymbol{r}'_S) \\ O_{ij} &= \int_I \mathrm{d}^3\boldsymbol{r}\ \chi_i^*(\boldsymbol{r})\chi_j(\boldsymbol{r}). \end{aligned} \tag{4}$$

H_{ij} is the matrix element of the Hamiltonian in region I, and the surface derivative terms ensure hermiticity. $(G_0^{-1})_{ij}$ is the matrix element of the embedding potential which converts the calculation for region I into one for region I embedded onto region II.

When the energy lies within the bulk continuum it is convenient to work in terms of the single-particle Green function rather than the wavefunctions. The Green function can be expanded in terms of our basis functions:

$$G(\boldsymbol{r}, \boldsymbol{r}'; E) = \sum_{ij} g_{ij}(E)\chi_i(\boldsymbol{r})\chi_j^*(\boldsymbol{r}') \tag{5}$$

where g_{ij} is given by the inhomogeneous matrix equation which can be written in matrix form:

$$\sum_k \left[H_{ik} + (G_0^{-1})_{ik} - E\,O_{ik}\right] g_{kj}(E) = \delta_{ij}. \tag{6}$$

The energy derivative terms do not appear in equation (6) as the embedding potential is evaluated at the energy at which the Green function is to be found. From the Green function, we can evaluate the local density of states (LDOS) which is the charge density of states at a particular energy:

$$\sigma(\boldsymbol{r}, E) = \sum_i |\psi_i(\boldsymbol{r})|^2 \delta(E - E_i) \tag{7}$$

or

$$\sigma(\boldsymbol{r}, E) = \frac{1}{\pi} \operatorname{Im} G(\boldsymbol{r}, \boldsymbol{r}; E + \mathrm{i}\epsilon). \tag{8}$$

With a knowledge of the LDOS, it then possible to calculate the charge density. This can be done by integrating σ over the occupied states which we do using contour integration making use of the analyticity of G in the upper half-plane. We use a semi-circular contour starting below the bottom of the valence band and ending up back on the real axis at E_F:

$$\rho(\boldsymbol{r}) = \frac{1}{\pi} \operatorname{Im} \int_C \mathrm{d}E\ G(\boldsymbol{r}, \boldsymbol{r}; E). \tag{9}$$

We use linearized augmented plane waves (LAPWs) as our basis; these are very accurate and convergence can often be achieved with as few as 50 LAPWs per atom. It is also very convenient to formulate the full potential in terms of LAPWs. For exchange and correlation we use the LDA [10] with the functional of Ceperley and Alder [11].

The embedding potential is obtained from a bulk (KKR) calculation using a relationship between embedding and the reflection properties of the substrate [8]. It is important to note that even though the KKR calculation employs a muffin-tin potential, in the surface calculation we calculate the full potential including warping terms in the interstitial region, non-spherical terms in the cores and non-planar terms in the vacuum. New developments in embedding mean that it is now possible to treat the substrate on the same footing as the surface region [12] and our future work will be carried out using these advances.

Details of the procedure that we use to iterate to self-consistency can be found in the paper by Inglesfield and Benesh [8]. In our study of Ag(001)c(2×2)–Xe we consider the effect of an applied electric field. This is brought into the calculation through a boundary condition on the solution of Poisson's equation: $\mathrm{d}V/\mathrm{d}z$ is set equal to the applied electric field deep in the vacuum. Using this condition, when we iterate to self-consistency we automatically get the surface screening charge, as the Fermi energy is fixed by the bulk and the substrate acts as a reservoir of electrons. In this work we use the conventional definition of the sign of the field; a positive field depletes the surface of electrons whereas a negative field increases the electron density, tending to pull the electrons into the vacuum.

3. The Ag(001) c(2 × 2)–Xe electronic structure

The field-free Xe/Ag(001) electronic structure has been calculated as described in section 2 using the surface embedded Green function (SEGF) code [8] in a two-layer (one Xe layer and one Ag layer) calculation. The calculations have been performed with the Xe atoms adsorbed in the c(2 × 2) structure at the 'on-top' sites. Adsorption at the on-top site is seen experimentally [13] and the c(2 × 2) structure is chosen for computational convenience. The atoms are situated such that the muffin tins touch, which results in a Xe–Xe spacing of 4.12 Å (a coverage of 5.89×10^{14} atoms cm^{-2}) and a Ag–Xe distance of 3.52 Å. Experimental values [14] give the Xe–Ag distance as ∼3.54 Å, in agreement with the distance that we use. A basis of 221 LAPWs was used with three special points in the irreducible part of the surface Brillouin zone. The charge density in a plane normal to the surface cutting through the centre of the atoms is shown in figure 2.

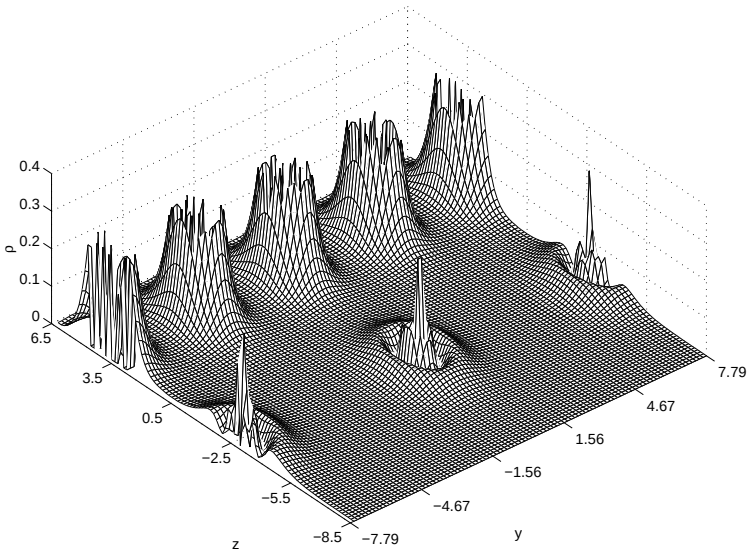

Figure 2. A surface plot of the Xe/Ag(001) valence charge density in a plane perpendicular to the surface.

Figure 3 shows the density of states at $\bar{\Gamma}$ in the different muffin tins of the system. We see as expected that the atomic Xe 5p levels become broadened and split into a $5p_z$, $5p_{x,y}$ doublet on adsorption. This is caused by the reduction in symmetry of the Xe atom when it is brought into the system. There are two possible mechanisms for this splitting: the interaction between the adsorbed Xe atom and the surface atoms, and two-dimensional band-structure effects within the Xe overlayer. We have identified the lower peak as being due to $5p_z$ and the upper peak as being due to $5p_{x,y}$. There is a third peak in between the two Xe 5p peaks; we have investigated this peak and have concluded that it is due to Ag orbitals penetrating into the Xe muffin tins. Comparing the DOS with our bulk Ag band structures, we have found that the peak is associated with a minimum in the band with Δ_1 symmetry at 0.95 au.

In experimental work, the Xe 5p level is seen to split into $5p_{1/2}$ and $5p_{3/2}$ levels. This is caused by spin–orbit coupling which we do not include. The $5p_{3/2}$ level splits further into $|m_j| = 1/2$ and $|m_j| = 3/2$ levels [15–18, 20] due to the reduction in symmetry in

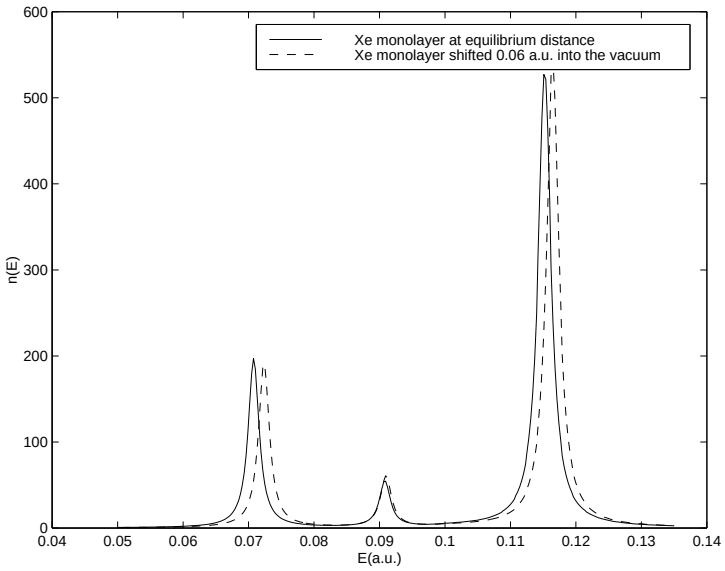

Figure 3. The p-resolved density of states inside the Xe muffin tins at $\bar{\Gamma}$.

analogy with the splitting observed in our calculations. The mechanism responsible for the splitting of the $5p_{3/2}$ peak which affects the energetic ordering of the $|m_j| = 1/2$ and $|m_j| = 3/2$ states has caused controversy as we mentioned earlier. Initially, both Ag–Xe and Xe–Xe interactions were put forwards as the mechanism causing the splitting, but later work identified Xe–Xe interactions as being the dominant effect [16, 18, 21–23]. This is in agreement with the work of Oxinos and Modinos [19] who in model calculations for singly adsorbed atoms saw an observable splitting due to the substrate only when the p level was below the valence band of the metal. From this, we would not expect to see splitting in calculations for Xe as the 5p orbital lies within the valence band of the metal substrate. To investigate the origin of the 5p splitting, we have performed calculations with the Xe overlayer displaced into the vacuum from the equilibrium position. If the splitting is due to Xe–Ag interactions then it should be affected by this displacement. What in fact we see in figure 3 is that the only effect of this displacement is to shift both of the peaks up in energy by the same amount. This suggests that the splitting is due to Xe–Xe interactions, in agreement with the general consensus in the literature. The splitting of order 1.3 eV which we observe is larger than that reported in the literature (for example 0.96 eV for Xe–Pt(111) [18]), but Cassuto and Ehrhardt [20] have shown that the splitting becomes larger as the Xe–Xe separation is reduced; the separation which we use in our geometry is smaller than those previously published (for example in the study of Xe–Pt previously mentioned, the Xe–Pt separation was 4.8 Å) and this explains why our splitting is greater than those seen in previously published work.

The Xe 5p peaks in our calculation are situated at around 4.2 eV below E_F, whereas spin-polarized photoemission data give them at approximately 5.5 eV below E_F [16]. This value is however in agreement with other *ab initio* calculations [24] and it can be explained in terms of the fact that we use the LDA without self-interaction corrections, and that we would expect these corrections to be substantial for the localized Xe wavefunctions. These corrections would lower the energy and hence our Xe states are at too high an energy.

Turning now to ground-state properties, our calculations give a workfunction of 4.21 eV,

a reduction of 0.46 eV compared to the value from our calculations for a clean Ag surface, for which $\phi = 4.67$ eV (in extremely good agreement with results from photoemission experiments [25]). The reduction of 0.46 eV in the workfunction is in agreement with experimental values which give the shift as 0.46 ± 0.06 eV [26, 27].

The reduction in workfunction occurs because of the interaction between the Xe monolayer and the substrate which causes a polarization of the adsorbate and a reduction in the surface potential barrier. The polarization of the adsorbate can be understood by considering the LDA picture put forward by Lang [40]. The electron density on the surface side of the adsorbate is higher than on the vacuum side leading to a deeper exchange–correlation hole which is more effective in lowering the energy of the adsorbate electrons. This means that it is energetically favourable for the adsorbate electrons to be in this region and hence the adsorbate becomes polarized.

Recently, support for Lang's LDA picture of rare-gas adsorption has appeared in the literature. The LDA approach leads to an exponential decay in the attractive force rather than the power-law dependence that the van der Waals mechanism would display. Helium diffraction experiments by Kirsten and Rieder [28] have demonstrated that the interaction potential of He with Pt(110)–(1 × 2) has an exponentially decaying attractive component when the He atom is close to the Pt surface.

4. Screening of applied electric fields

When an electric field is applied to a metal surface, the electrons respond by screening the field and prevent it from penetrating into the metal. The main aim of this work is to study this screening and to say what (if any) effect it has on the interaction between the adsorbates and the substrate. In addition to this motivation, we can use the screening charge to deduce the position of the centre of gravity of the screening charge and the field dependence of this quantity [29] which has ramifications for second-harmonic generation (SHG) as we shall see later in this section.

Table 1. The induced screening charge density ρ_{ind} and the induced screening charge density corresponding to perfect screening ρ_{perfect}.

E	ρ_{ind}	ρ_{perfect}
−0.010	−0.000 774	−0.000 795
−0.005	−0.000 388	−0.000 398
0.005	0.000 387	0.000 398
0.010	0.000 775	0.000 795
0.020	0.001 553	0.001 591

We have applied fields ranging from −0.01 au to 0.02 au (with the sign convention as defined in section 2) to the system† and evaluated the total induced screening charge at each field strength. The calculation gives perfect screening (which corresponds to a surface charge of $E/(4\pi)$ per unit area) to within 2% as can be seen in table 1.

When we consider the distribution of the screening charge, we find an extremely rich structure. Initially we concentrate on the planar-averaged screening charge which is defined

† Where one atomic unit (1 au) $= 5.14 \times 10^{11}$ V m^{-1}.

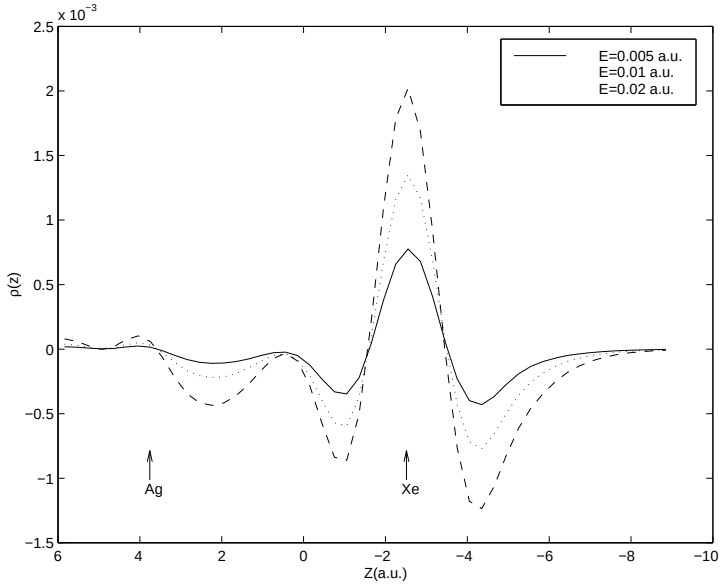

Figure 4. The planar-averaged screening charge for $E = 0.005$, 0.01 and 0.02 au. The bulk is to the left of the figure and vacuum is to the right.

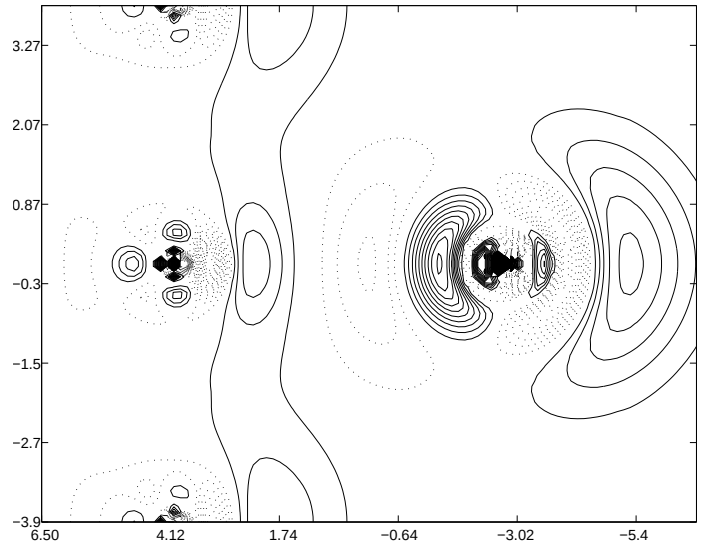

Figure 5. A contour plot of the screening charge induced by a field of 0.01 au. The plot is on a plane in the same orientation as figure 2. The solid contours show where electronic charge is lost; the dotted ones show where electronic charge is gained. The Xe atom is centred at $z = -2.75$ au, the Ag atoms at $z = 3.9$ au.

as follows:

$$\rho_{\mathrm{ind}}(z) = \frac{1}{\mathcal{A}} \int_{\mathcal{A}} \mathrm{d}^2 \boldsymbol{r}\ \rho_{\mathrm{ind}}(\boldsymbol{r}) \tag{10}$$

where $\rho_{\mathrm{ind}}(\boldsymbol{r})$ is $\rho_{E\neq 0}(\boldsymbol{r}) - \rho_{E=0}(\boldsymbol{r})$ and $\mathcal{A}$ is the area of the unit cell. We see, as shown in figure 4, that just outside the Ag atoms a layer of screening charge builds up which prevents the field from entering the metal. Around the Xe atom the planar-averaged screening charge has a dipole-like profile. If we now consider the contour plot of the screening charge shown in figure 5 the rich structure of the screening charge begins to reveal itself. Again as with the planar-averaged screening charge, we see a layer of screening charge sited just above the metal atoms but now we see that it bends around the ion cores as observed by Aers and Inglesfield [29, 30]. These authors initially postulated that this was due to the repulsive pseudopotential of the Ag core, but it later became apparent that the same effect was observed in Al where the pseudopotential is attractive, so clearly more thought has to go into obtaining the mechanism behind this effect. There is also a very interesting polarization effect inside the ion cores which was also observed by Aers and Inglesfield for clean Ag and Al.

When we look at the Xe atoms, we again see the dipole-like polarization which was also evident in figure 4 but now the rich structure contained within this polarization becomes apparent. From figures 4 and 5 we can see that there is some redistribution of charge in the system and we see that the Xe becomes polarized (in fact more polarized if we go back to Lang's picture of adsorption). What we cannot tell, however, is whether there is any charge transfer (and hence field-induced chemisorption). We will address this problem in the next section.

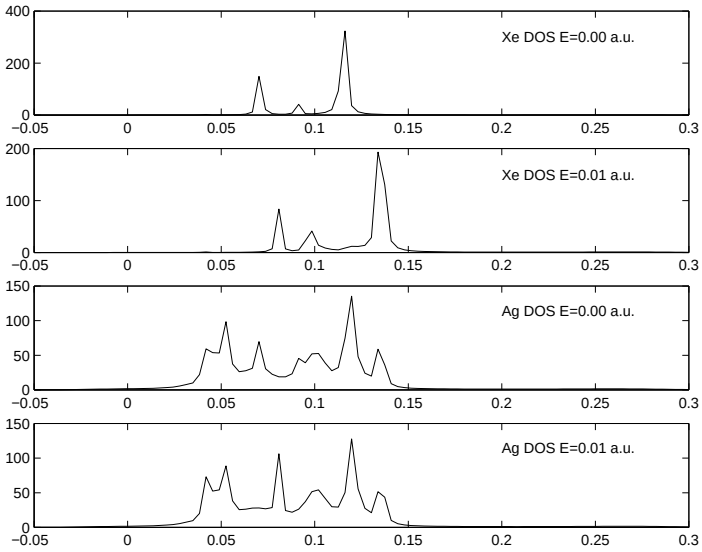

Figure 6. Densities of states for zero applied field and for a 0.01 au applied field at $\bar{\Gamma}$.

It is informative to look at the effect of applied fields on the DOS (figure 6) on each atom (where by 'Xe DOS' for example we mean the local density of states integrated through the Xe muffin tin), as this gives further insight into the nature of the screening. Looking at the top two plots which show the Xe DOS for zero field and a 0.01 au field, we can see that applying a positive field shifts all of the Xe states upwards in energy. Turning to the lower two plots which show the Ag DOS, it seems that there are no shifts in the Ag DOS. This is intuitively correct as the field is screened near the top of the Ag atoms whereas it is essentially unscreened in the Xe monolayer. However, on closer examination it becomes

clear that there is a peak at about 0.07 au which shifts to 0.08 au when the field is applied. This peak in fact corresponds to the Xe $5p_z$ state, which extends slightly into the Ag layer and appears in the Ag DOS. So by considering the densities of states, we again come to the conclusion that the screening in the system is so good as to be virtually perfect for the Ag atoms, whereas the applied field shifts the states of the adsorbate up in energy.

A useful measure of the screening charge is the image plane (z_0) which is the centre of gravity of the induced screening charge. By considering how the image plane varies when a field is applied we can find out information about how the screening charge is redistributing itself when the field is varied. We can obtain the position of the image plane using the planar-averaged induced charge density ρ_{ind}. We can then find the position of z_0 (measured relative the jellium edge, i.e. half an interatomic spacing from the last atomic plane of Ag):

$$z_0 = \left(\int \mathrm{d}z\ z\rho_{\mathrm{ind}}(z)\right) \Big/ \left(\int \mathrm{d}z\ \rho_{\mathrm{ind}}(z)\right). \tag{11}$$

Now previous calculations [29] for clean Ag surfaces have reported that the position of the image plane depended linearly on the applied electric field with the following dependence:

$$z_0(E) = -0.97 + 8.83E \qquad \text{(in atomic units)}. \tag{12}$$

We find that the adsorption of a monolayer of Xe modifies this behaviour, and introduces a quadratic dependence (figure 7) which can be fitted by

$$z_0(E) = -5.29 + 3.19E - 123.84E^2 \qquad \text{(in atomic units)}. \tag{13}$$

The field dependence of z_0 corresponds to non-linear screening, even though the total screening charge is proportional to the applied field from perfect screening. For a low-frequency field, it contributes to the longitudinal second-harmonic current normal to the surface [31]. The coefficient of E is proportional to the quadratic response and so we can see from equations (12) and (13) that adsorption of a monolayer of Xe reduces this response, and hence the second-harmonic signal.

Using the fits obtained above (equations (12) and (13)) we can obtain the low-field limit for the position of the image plane and so can estimate the adsorbate-induced shift of the image plane. The classical shift of the image plane Δz caused by a thin dielectric layer of thickness d and static dielectric constant ϵ is [32]

$$\Delta z = -\frac{\epsilon - 1}{\epsilon} d. \tag{14}$$

Our dielectric layer is 7.79 au thick, and if we use the static dielectric constant for solid Xe, $\epsilon = 2.09$ [33], we find from (14) that the classical shift of the image plane is -4.06 au which agrees extraordinarily well with the distance of -4.31 au that we find in our calculation. This means that apparently just a single monolayer of dielectric exhibits bulk dielectric properties!

5. Effective charge and screening charge

We now present a generalization of the concept of effective charge [34] to arbitrary fields and use it to study the nature of the bonding of the Xe adsorbate to the Ag substrate and the effect of applied fields on this bonding. The generalized effective charge is related to the force on individual surface atoms due to applied fields and it allows us to associate screening charge with individual atoms. In the limit of low fields, the force normal to the surface on atoms of type i in a field is [34–37]:

$$F_i = q_i^* E \tag{15}$$

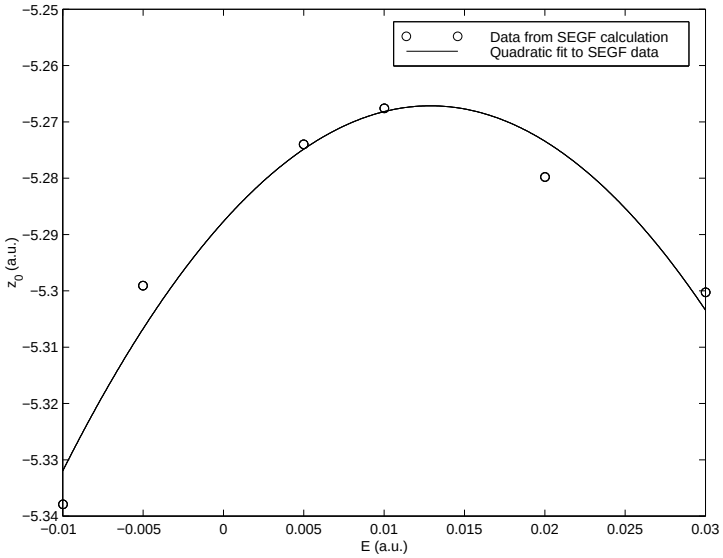

Figure 7. The quadratic relationship between the applied field and the position of the image plane. The circles are the results of our calculation; the line is a quadratic fit to the data.

where q_i^* is the effective charge and E is the unscreened external electric field. The effective charge also gives the change in the surface dipole contribution to the workfunction when atoms of type i are displaced by $\mathrm{d}z_i$ perpendicular to the surface [34, 37]:

$$\frac{\partial \phi}{\partial z_i} = -\frac{4\pi q_i^*}{A_i} \tag{16}$$

where A_i is the area per atom. (In this section, we take positive z as pointing out of the surface to remain consistent with our other paper [9].)

Although the effective charge gives us the force on the atoms in a field, the definition in (16) in terms of change in surface dipole moment shows that we cannot necessarily associate it with charge transfer between atoms. As we shall see later, a van der Waals treatment of the distance dependence of the Xe dipole can lead to an effective charge in good agreement with our calculations without any charge transfer as such. However, the effective charge does have properties associated with real charges as well as giving the force. For example, the sum of the effective charges is zero; otherwise there would be a force on a surface in a uniform field linear in the field (in the low-field limit) which is not the case. Moreover, charge transfer is an arbitrary quantity, whereas the force on a surface atom is well defined. We should emphasize that (15) gives the total force on an atom in the field including all quantum mechanical effects and self-consistent screening. It is not just classical electrostatics.

Let us now consider the generalization of the concept of effective charge to allow us to calculate the force on an atom at the surface in an arbitrary field, restricting ourselves to metallic surfaces for which perfect screening applies. We use an extension of the classical argument for finding the force on the plates of a parallel-plate capacitor. One plate is the surface, whilst the other is an arbitrary electrode. The potential of the electrode is initially V with respect to the surface which is fixed at zero potential. On taking charge $\mathrm{d}q$ from

the electrode to the surface, the energy change of the system is $\mathrm{d}U$, with

$$V = -\frac{\partial U}{\partial q}. \tag{17}$$

If we now move the atoms of type i by $\mathrm{d}z_i$, the potential across the capacitor changes in just the same way as the workfunction changes in the field-free case. From (17),

$$\frac{\partial V}{\partial z_i} = -\frac{\partial^2 U}{\partial q\, \partial z_i}. \tag{18}$$

But $-\partial U/\partial z_i$ is the total force on the atoms of type i, so (18) becomes

$$\frac{\partial V}{\partial z_i} = N_i \frac{\partial F_i}{\partial q} \tag{19}$$

where F_i is the force on each atom of type i, and there are N_i of these atoms on the entire surface. Replacing $\mathrm{d}q$ by the change in electric field $\mathrm{d}E$ between the plates, we obtain a relationship between $\partial F_i/\partial E$ and $\partial V/\partial z_i$:

$$\frac{\partial F_i}{\partial E} = \frac{A_i}{4\pi} \frac{\partial V}{\partial z_i}. \tag{20}$$

We can easily evaluate the right-hand side of this expression by performing an electronic structure calculation in the presence of an electric field. We simply shift the atoms of type i by $\mathrm{d}z_i$ and see how much the vacuum potential shifts. It is natural to define $\partial F_i/\partial E$ as the charge $\mathcal{Q}_i$ on atom i which can be determined very straightforwardly from the right-hand side of equation (20). The difference in sign between (16) and (20) arises because V is the electrostatic potential whilst ϕ is an electron potential energy. Again F_i includes all quantum mechanical effects.

The effective charge $\mathcal{Q}_i$ is related to the change in dipole moment of the surface charge when atoms of type i are moved. Keeping the potential inside the solid fixed, Poisson's equation tells us that the change in potential outside the surface when atoms i are moved a distance $\mathrm{d}z_i$ is given by

$$\frac{\partial V}{\partial z_i} = \frac{4\pi}{\mathcal{A}} \int_{-\infty}^{\infty} \mathrm{d}z \int_{\mathcal{A}} \mathrm{d}^2\boldsymbol{r}\; z \frac{\partial \rho(\boldsymbol{r})}{\partial z_i} \tag{21}$$

where $\rho(\boldsymbol{r})$ is the charge density and the two-dimensional integral is over the unit cell with area $\mathcal{A}$. From the definition of effective charge it follows that

$$\mathcal{Q}_i = \frac{1}{\mathcal{N}_i} \int_{-\infty}^{\infty} \mathrm{d}z \int_{\mathcal{A}} \mathrm{d}^2\boldsymbol{r}\; z \frac{\partial \rho(\boldsymbol{r})}{\partial z_i} \tag{22}$$

where $\mathcal{N}_i$ is the number of atoms of type i in the unit cell. A sum rule immediately follows from this. If we move all of the atoms by δz, the change in charge density is just a shift in the whole system, so

$$\delta\rho(\boldsymbol{r}) = \delta z \sum_i \frac{\partial \rho}{\partial z_i} = \rho(z - \delta z) - \rho(z) \tag{23}$$

and

$$\sum_i \mathcal{N}_i \mathcal{Q}_i = \frac{1}{\delta z} \int_{-\infty}^{\infty} \mathrm{d}z \int_{\mathcal{A}} \mathrm{d}^2\boldsymbol{r}\; z\,[\rho(z - \delta z) - \rho(z)] = \int_{-\infty}^{\infty} \mathrm{d}z \int_{\mathcal{A}} \mathrm{d}^2\boldsymbol{r}\; \rho(\boldsymbol{r}). \tag{24}$$

Hence we obtain

$$\sum_i \mathcal{N}_i \mathcal{Q}_i = \mathcal{Q} \tag{25}$$

where $\mathcal{Q}$ is the total charge per surface unit cell—this is zero if there is no electric field, and is the screening charge in the presence of a field.

Let us separate $\mathcal{Q}_i$ into the zero-field effective charge q^* and a term linear in the applied field—in other words, we consider the first two terms in a Taylor series:

$$\mathcal{Q}_i = q_i^* + \alpha_i E. \tag{26}$$

Then from equation (20) we can see that the force on atom i is given by

$$F_i = q_i^* E + \frac{1}{2}\alpha_i E^2. \tag{27}$$

Summing over all atoms we are left with the quadratic term only as we know from simple electrostatics. So the second term in (26) allows us to associate screening charge with individual atoms. To find $\mathcal{Q}_i$, all we have to do is move the relevant atom and obtain the shift in the vacuum level from our self-consistent calculations.

6. Effective charge and Xe–Ag bonding

We have calculated the generalized effective charge $\mathcal{Q}_i$ for the Xe–Ag system for different applied electric fields as shown in table 2. Firstly we consider the field-free case where we see that q^*_{Xe} is $-0.090|e|$. This is largely counterbalanced by the effective charge on the Ag atom directly below the Xe, $q^*_{\mathrm{Ag1}} = +0.086|e|$. This demonstrates the effectiveness of metallic screening of perturbations due to the adsorbate and is in agreement with the description given by Kreuzer [38] with the adsorbate interacting predominantly with the atom above which it is adsorbed.

Table 2. The effective charge on each of the atoms as a function of the applied electric field. The Xe atoms are adsorbed above atom Ag1. $\mathcal{Q}$ is the screening charge obtained from the sum of the effective charges, and $\mathcal{Q}_{\mathrm{perfect}}$ is the screening charge corresponding to perfect screening.

E	$\mathcal{Q}_{\mathrm{Xe}}$	$\mathcal{Q}_{\mathrm{Ag1}}$	$\mathcal{Q}_{\mathrm{Ag2}}$	$\mathcal{Q}$	$\mathcal{Q}_{\mathrm{perfect}}$
0.000	−0.0932	+0.0858	+0.0017	−0.0057	+0.0000
0.005	−0.0893	+0.0994	+0.0082	+0.0183	+0.0242
0.010	−0.0840	+0.1149	+0.0157	+0.0466	+0.0482
0.020	−0.0691	+0.1359	+0.0312	+0.0980	+0.0966

These calculated effective charges suggest that there is some chemisorptive nature to the Xe–Ag bond and Mingo *et al* [39] attributed this to the overlap of the broadened unoccupied Xe 6s orbital with the Fermi energy which leads to partial occupation of this orbital. These authors found a transfer of $-0.1|e|$ of real charge from the substrate to the Xe, in good agreement with the effective charge which we have calculated. Lang [40] has already shown that an LDA approach works for adsorption of rare-gas atoms on a jellium surface and stressed that the overlap of the Xe electron distribution with the substrate electron gas is important for bonding. However, we must remember that the effective charge is not necessarily a real charge, even though it gives the force on an atom in an electric field. An effective charge corresponds to a variation in surface dipole moment with atomic displacement and this can occur by a purely van der Waals mechanism.

A van der Waals treatment predicts that the dipole moment varies as $(z_{\mathrm{Xe}} - z_{\mathrm{VdW}})^{-4}$ [40], where z_{VdW} is the position of the van der Waals reference plane. This means that as we move

the adsorbate into vacuum, the dipole moment decreases, which corresponds to negative effective charge on the Xe atoms. This approach gives

$$q^*_{\mathrm{Xe}} = \frac{A_i}{\pi}\frac{\Delta\phi}{(z_{\mathrm{Xe}} - z_{\mathrm{VdW}})}. \tag{28}$$

Taking $z - z_{\mathrm{VdW}} = 4.2$ au [41], $A_i = 60.7$ au and using the change in workfunction on Xe adsorption obtained from our self-consistent calculations ($\Delta\phi = -0.46$ au) yields an effective charge of $-0.08|e|$ which is in excellent agreement with our first-principles calculations. This agreement is surprising, because our value of q^* is found in a LDA calculation of dipole moments, whereas the van der Waals values come from non-local exchange–correlation effects.

We now turn to the effect of an applied electric field. From table 2 we see that the sum of the generalized effective charges $\mathcal{Q}$ agrees well with perfect screening. The screening charge is predominantly on the Ag atoms, with the Ag atoms sitting under the Xe adsorbates responding almost twice as much to the applied field as the Ag atoms not covered by the Xe atoms. There are several different ways of interpreting this effect. We would expect the valence wavefunctions of the Ag atoms under the Xe to penetrate further into vacuum as the electrons see a reduced tunnelling barrier at the adsorbed Xe [42]; this would lead to them responding more strongly to the field. Figure 8 shows the Ag valence charge density along lines through the centre of the Xe atoms and in between the Xe atoms; it shows that at the Xe atoms, the Ag valence wavefunctions penetrate much further into the vacuum than in the absence of Xe atoms and so supports this idea.

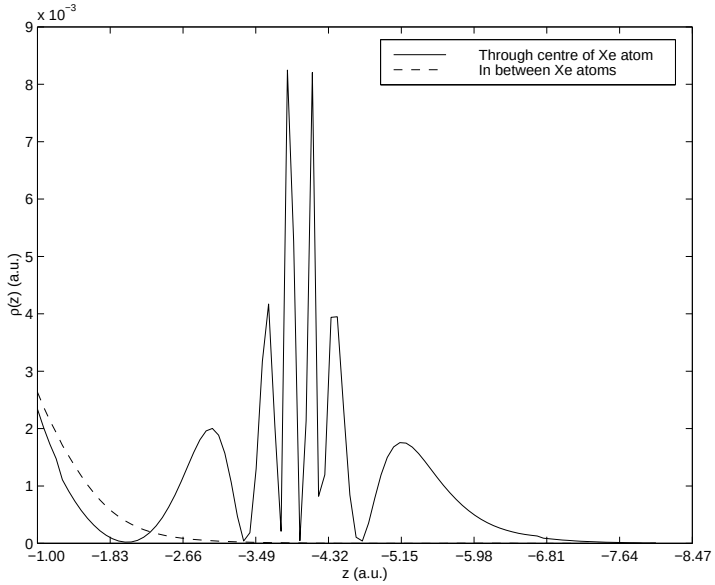

Figure 8. The Ag valence charge density plotted on lines through the centre of the Xe adsorbate and in between the Xe adsorbates to show the effect of the adsorbate on the penetration of the wavefunction into the vacuum. The Ag charge density is separated from the Xe charge density by plotting the charge density for electrons near to the Fermi energy (which is at 0.25 au) where the contribution from Xe is negligible.

As the field increases, the generalized effective charge of the Xe atom becomes less negative. This may be connected with the charge transfer found by Kreuzer and co-workers

in model studies of inert-gas adsorbates in an electric field—the electric field raises the energy levels on the adsorbate, which consequently tend to empty. This charge transfer has been linked by Kreuzer to the increased bonding of inert-gas atoms to metal surfaces in the presence of electric fields—a phenomenon which they have termed field-induced chemisorption [38].

7. Field desorption and the atomic switch

To study the processes occurring in field desorption, the results shown in table 2 have been extended for fields up to 0.06 au, and are fitted by the formula

$$\mathcal{Q}_{\mathrm{Xe}} = -0.097 + 1.165E + 23.147E^2 \qquad \text{(in atomic units)}. \tag{29}$$

It then follows from equation (20) that

$$F_{\mathrm{Xe}} = -0.097E + 0.0583E^2 + 7.715E^3 \qquad \text{(in atomic units)}. \tag{30}$$

From this we can see that for small positive fields (which push electrons away into the bulk) the Xe atoms are pushed towards the substrate. Initially, this force increases with increasing field but then begins to decrease, changing sign at around 0.08 au after which the field pulls the Xe atom away from the surface into the vacuum. It is important to emphasize again that this is the total force on the Xe atom at a fixed position (in this case the zero-field equilibrium position) including all field-induced bonding and charging effects. What actually happens at a real surface is that the adsorbate atom moves under the influence of the force until there is no net force on the atom; we should also note that E is the uniform field above the surface, but all local field enhancement is included implicitly in our method.

The negative force pushing the Xe towards the surface at low fields is associated with the field-induced chemisorption mentioned above. The potential energy curves of Nath *et al* [43] for inert-gas atoms adsorbed upon metal surfaces show a force towards the surface at low fields in agreement with this study, along with a deepening of the adsorption potential well which moves closer to the surface. This is field-induced chemisorption. Nath *et al* also saw that as the field is increased, the force on an atom at the equilibrium position changes sign in agreement with our work. Due to the rapid variation of F_{Xe} at large E we expect that a field somewhat larger than 0.08 au (4.1 V Å^{-1}) will overcome the van der Waals and other bonding forces to strip the adsorbed atom from the surface. This is certainly an overestimate of the field required for field evaporation as we have not considered non-adiabatic effects such as the ionization reaction $\mathrm{Xe} \rightarrow \mathrm{Xe}^+ + \mathrm{e}^-$.

A subject that has seen a great deal of attention in recent times is the manipulation of adsorbates with electric fields. In particular we consider the Eigler switch [4], in which the application of a positive field to an STM tip causes Xe atoms to jump from a Ni surface to the STM tip. Under typical working conditions, the tip is biased to +0.8 V and is situated about 4 Å from the surface. This corresponds to an electric field of −0.004 au using our convention for signs. Now it can be shown from binding energy curves that the force needed to remove Xe adsorbed on Ag is about 100–150 meV Å^{-1} [39, 45]. From our calculations, the force due to the fields in the work of Eigler *et al* is only about 4×10^{-4} au (20 meV Å^{-1}). What becomes clear from these results is that the desorption mechanism cannot be purely adiabatic. The most important effect is probably thermal activation due to the non-adiabatic vibrational heating from inelastic electron tunnelling [44]. However, the force on the effective charge does play an important role insofar as it produces a bias-dependent shift of the potential well of the Xe adsorbate on the STM tip relative to the well for adsorption on the surface. This means that the energy required (from the inelastic

tunnelling effects) to make the atom jump between the wells becomes less and so can occur with less thermal activation. From this we can see that the bias required to make the atom jump is determined by the interplay between the shift of the adsorption well and the energy supplied by the inelastic tunnelling effects.

References

[1] Suchorski Y U, Ernst N, Schmidt A, Medvedev V K, Kreuzer H J and Wang R L C 1996 *Prog. Surf. Sci.* **53** 135
[2] Wang R L C, Kreuzer H J and Forbes R G 1996 *Surf. Sci.* **350** 183
[3] Eigler D M and Schweizer E K 1990 *Nature* **344** 524
[4] Eigler D M, Lutz C P and Rudge W E 1991 *Nature* **352** 600
[5] Kingham D R 1986 *J. Physique Coll.* **47** C2 11
[6] Shima N and Tsukada M 1987 *J. Physique Coll.* **49** C6 91
[7] Aberenkov I V and Bar'yudin L E 1992 *J. Phys.: Condens. Matter* **4** 2239
[8] Inglesfield J E and Benesh G A 1988 *Phys. Rev.* B **31** 6682
[9] Clarke S, Inglesfield J E, Nekovee M and de Boer P K 1998 *Phys. Rev. Lett.* **80** 3571
[10] Lundqvist S and March N H 1983 *Theory of the Inhomogeneous Electron Gas* (New York: Plenum)
[11] Ceperley D M and Alder B J 1980 *Phys. Rev. Lett.* **45** 566
[12] van Hoof J B A N 1997 *Thesis* Catholic University of Nijmegen
[13] Eigler D M 1997 private communication
[14] Unguris J, Bruch L W, Moog E R and Webb M B 1979 *Surf. Sci.* **87** 415
[15] Waclawski B J and Herbst J F 1975 *Phys. Rev. Lett.* **35** 1594
[16] Schönhense G, Eyers A, Friess U, Schäfers F and Heinzmann U 1985 *Phys. Rev. Lett.* **54** 547
[17] Horn K, Scheffler M and Bradshaw A M 1978 *Phys. Rev. Lett.* **41** 822
[18] Schönhense G 1986 *Appl. Phys.* A **41** 39
[19] Oxinos G and Modinos A 1979 *Surf. Sci.* **89** 292
[20] Cassuto A and Ehrhardt J J 1988 *J. Physique* **49** 1753
[21] Vogt B, Kessler B, Müller N, Schönhense G, Schmiedeskamp B and Heinzmann U 1991 *Phys. Rev. Lett.* **67** 1318
[22] Erskine J L 1981 *Phys. Rev.* B **24** 2236
[23] Kambe K 1981 *Surf. Sci.* **105** 95
[24] Crampin S, unpublished results
[25] *AIP Physics Vade-mecum* 1981 (New York: American Institute of Physics)
[26] Merry W R, Jordan R E, Padowitz D F and Harris C B 1993 *Surf. Sci.* **295** 393
[27] Ishi S and Viswanathan B 1991 *Thin Solid Films* **201** 373
[28] Kirsten E and Rieder K H 1989 *Surf. Sci.* **242** L857
[29] Aers G C and Inglesfield J E 1989 *Surf. Sci.* **217** 367
[30] Inglesfield J E 1990 *Vacuum* **41** 543
[31] Weber A and Liebsch A 1987 *Phys. Rev.* B **36** 6411
[32] Nekovee M 1997 private communication
[33] Leadbetter A J and Thomas H E 1964 *Trans. Faraday Soc.* **61** 10
[34] Colbourn E A and Inglesfield J E 1991 *Phys. Rev. Lett.* **66** 2006
[35] Trullinger S E and Cunningham S L 1973 *Phys. Rev.* B **8** 2622
[36] Mills D L 1977 *Prog. Surf. Sci.* **8** 143
[37] Hamann D R 1987 *J. Electron Spectrosc.* **44** 1
[38] Kreuzer H J 1988 *J. Physique Coll.* **49** C6 7
[39] Mingo N, Jurczyszyn L, Garcia-Vidal F J and Saiz-Pardo R 1996 *Phys. Rev.* B **54** 2225
[40] Lang N D 1981 *Phys. Rev. Lett.* **46** 842
[41] Zaremba E and Kohn W 1976 *Phys. Rev.* B **13** 2270
[42] Eigler D M, Weiss P S, Schweizer E K and Lang N D 1991 *Phys. Rev. Lett.* **66** 118
[43] Nath K, Kreuzer H J and Anderson A B 1986 *Surf. Sci.* **176** 261
[44] Gao S, Persson M and Lundqvist B I 1997 *Phys. Rev.* B **55** 4825
[45] Bouju X, Joachim C, Girard C and Sautet P 1993 *Phys. Rev.* B **47** 7454